
MANAS: Multi-Agent Neural Architecture Search

| | | | |
|-------------------------------|--------------------------|--------------------|---------------------|
| Fabio Maria Carlucci * | Pedro M Esperança | Marco Singh | Antoine Yang |
| Noah's Ark Lab | Noah's Ark Lab | Noah's Ark Lab | Noah's Ark Lab |
| Huawei, London | Huawei, London | Huawei, London | Huawei, London |
| | | | |
| Victor Gabillon | Xang Xu | Zewei Chen | Jun Wang |
| Noah's Ark Lab | Noah's Ark Lab | Noah's Ark Lab | Noah's Ark Lab |
| Huawei, London | Huawei, Hong Kong | Huawei, Hong Kong | Huawei, London |

Abstract

The Neural Architecture Search (NAS) problem is typically formulated as a graph search problem where the goal is to learn the optimal operations over edges in order to maximise a graph-level global objective. Due to the large architecture parameter space, efficiency is a key bottleneck preventing NAS from its practical use. In this paper, we address the issue by framing NAS as a multi-agent problem where agents control a subset of the network and coordinate to reach optimal architectures. We provide two distinct lightweight implementations, with reduced memory requirements (1/8th of state-of-the-art), and performances above those of much more computationally expensive methods. Theoretically, we demonstrate vanishing regrets of the form $\mathcal{O}(\sqrt{T})$, with T being the total number of rounds. Finally, aware that random search is an, often ignored, effective baseline we perform additional experiments on 3 alternative datasets and 2 network configurations, and achieve favourable results in comparison.

1 Introduction

Determining an optimal architecture is key to accurate deep neural networks (DNNs) with good generalisation properties (Szegedy et al., 2017; Huang et al., 2017; He et al., 2016; Han et al., 2017; Conneau et al., 2017; Merity et al., 2018). Neural architecture search (NAS), which has been formulated as a graph search problem, can reduce the need for application-specific expert designers allowing for a wide-adoption of sophisticated networks in various industries. Zoph and Le (2017) presented the first modern algorithm automating structure design, and showed that resulting architectures can indeed outperform human-designed state-of-the-art convolutional and recurrent networks (Ko, 2019; Liu et al., 2019). Though holding the promise of flexible architectures, NAS problems are domain-specific with search spaces tailored to particular applications. In image classification, for instance, pursuing optimal convolutional architectures is reduced to searching for the best convolutional filters, pooling operations, and fully connected layers in a convolutional neural network (CNN). Unfortunately, even when only considering these operations, NAS problems are still computationally intensive with results reporting hundreds or thousands of GPU-days for discovering state-of-the-art architectures (Zoph and Le, 2017; Real et al., 2017; Liu et al., 2018a,b).

Research efforts produced a wealth of techniques ranging from reinforcement learning, where a controller network is trained to sample promising architectures (Zoph and Le, 2017; Zoph et al., 2018; Pham et al., 2018), to evolutionary algorithms that evolve a population of networks for optimal DNN design (Real et al., 2018; Liu et al., 2018b). Alas, these approaches are inefficient and can be extremely computationally and/or memory intensive as some require all tested architectures to

*[fabio.maria.carlucci/pedro.esperanca/victor.gabillon/chen.zewei/w.j]@huawei.com.

be trained from scratch. It is worth noticing that weight-sharing, as introduced in ENAS (Pham et al., 2018), can alleviate this. Even so, these techniques cannot easily scale to large data-sets, e.g., ImageNet. Recently, however, novel gradient-based frameworks enabled more efficient solutions by introducing a continuous relaxation of the search space. DARTS (Liu et al., 2019), for example, uses this relaxation to optimise architecture parameters using gradient descent in a bi-level optimisation problem, while SNAS (Xie et al., 2019) updates architecture parameters and network weights under one generic loss. Still, due to memory constraints the search has to be performed on 8 cells, which are then stacked 20 times for the final architecture. This solution is a coarse approximation to the original problem as we show in Section 5. In fact, we show that searching directly over 20 cells leads to a reduction in test-error (0.24 p.p.; 8% relative to Liu et al., 2019). ProxylessNAS (Cai et al., 2019) is one exception, as it can search for the final models directly; nonetheless they still require twice the amount of memory used by our proposed algorithm.

To enable the possibility of large-scale joint optimisation of deep architectures, we contribute the first multi-agent learning algorithm for neural architecture search: MANAS. Our algorithm combines the memory and computational efficiency of multi-agent systems, which is achieved through action coordination with the theoretical rigour of online machine learning, allowing us to balance exploration versus exploitation. Due to its distributed nature, MANAS enables large-scale optimisation of deeper networks while learning different operations per-cell. Theoretically, we demonstrate that using different sampling schemes, MANAS implicitly coordinates learners to recover vanishing regrets, guaranteeing convergence. Empirically, we show that our method achieves state-of-the-art accuracy results with significant reductions in memory (1/8th of Liu et al., 2019) and computational time. To minimise algorithmic overfitting and provide an unbiased evaluation of NAS methods, we propose three new data sets which have been historically used in the CV literature. Finally, we confirm concerns raised in Sciuto et al. (2019) and Li and Talwalkar (2019) claiming that current algorithms often achieve minor gains over random architectures. We demonstrate, however, that MANAS still produces competitive results when considering limited computational budgets.

In short, our contributions can be summarised as: 1) framing NAS as a multi-agent learning problem where each agent supervises a subset of the network; agents coordinate through a credit assignment technique which infers the quality of each operation in the network, without suffering from the combinatorial explosion of potential solutions. 2) Proposing two lightweight implementations of our framework which exploit sparse architecture search: our algorithms are computationally and memory efficient, and achieve state-of-the-art results on Cifar-10 and ImageNet when compared with competing methods; furthermore MANAS allows search *directly* on large scale datasets. 3) Presenting 3 news datasets for NAS evaluation and offer a fair comparison with random architectures.

2 Preliminary: Neural Architecture Search

We consider the NAS problem as formalised in DARTS (Liu et al., 2019). At a higher level, the architecture is composed of a *computation cell* that is a building block meant to be learned and stacked in the network. This cell processes the inputs in a sequential but very general fashion, and can be represented by a directed acyclic graph (DAG) with V nodes and N edges, where edges connect all nodes i, j from i to j where $i < j$. Each vertex $\mathbf{x}^{(i)}$ is a latent representation for $i \in \{1, \dots, V\}$. Each directed edge (i, j) (with $i < j$) is associated with some operation $o^{(i,j)}$ that transforms $\mathbf{x}^{(i)}$. Intermediate node values are computed based on all of its predecessors as $\mathbf{x}^{(j)} = \sum_{i < j} o^{(i,j)}(\mathbf{x}^{(i)})$.

For each edge connecting two nodes (i, j) , an architect needs to intelligently select one elementary operation $o^{(i,j)}$ from a finite set of K operations $\mathcal{O} = \{o_k(\cdot)\}_{k=1}^K$, where each operation represents some function to be applied to $\mathbf{x}^{(i)}$ to compute $\mathbf{x}^{(j)}$, e.g., convolutions, pooling and averaging layers. To each $o_k^{(i,j)}(\cdot)$ is associated a set of operational weights $w_k^{(i,j)}$ that needs to be learned. For instance in the case where $o_k^{(i,j)}(\cdot)$ is a convolution operation, $w_k^{(i,j)}$ would represent the weights of the filter.

Additionally, a parameter $\alpha_k^{(i,j)} \in \mathbb{R}$ characterises the importance of operation k within the pool \mathcal{O} for each edge (i, j) . The sets of all the operational weights $\{w_k^{(i,j)}\}$ and architecture parameters

$\{\alpha_k^{(i,j)}\}$ are denoted by \mathbf{w} and α , respectively. DARTS defined the operation $\bar{o}^{(i,j)}(\mathbf{x})$ as

$$\bar{o}^{(i,j)}(\mathbf{x}) = \sum_{k=1}^K \frac{e^{\alpha_k^{(i,j)}}}{\sum_{k'=1}^K e^{\alpha_{k'}^{(i,j)}}} \cdot o_k^{(i,j)}(\mathbf{x}) \quad (1)$$

in which α encodes the network architecture. The optimal choice of architecture is defined by the pair $(\alpha^*, \mathbf{w}^*(\alpha))$ that solves

$$\min_{\alpha} \mathcal{L}^{(\text{val})}(\alpha, \mathbf{w}^*(\alpha)) \quad \text{s.t.} \quad \mathbf{w}^*(\alpha) = \arg \min_{\mathbf{w}} \mathcal{L}^{(\text{train})}(\alpha, \mathbf{w}). \quad (2)$$

where \mathbf{w} is optimised on the training loss while α is optimised on the validation loss. The final objective is to obtain a *sparse* architecture $\mathcal{Z}^* = \{\mathcal{Z}^{(i,j)}\}, \forall i, j$ where $\mathcal{Z}^{(i,j)} = [z_1^{(i,j)}, \dots, z_K^{(i,j)}]$ with $z_k^{(i,j)} = 1$ for k corresponding to the best operation and 0 otherwise. That is, for each pair (i, j) a *single operation* is selected.

3 Online Multi-agent Learning for AutoML

We formalise NAS using a multi-agent (MA) learning problem, where a set of agents—each selecting edge operations in the DAG—collaborate to discover optimal architectures. Not only will such a framework allow for scalable and efficient solutions (see Section 4), but will also enable a rigorous theoretical foundation. Before commencing with our exact solution, however, we next survey problems from gradient-based NAS to motivate our choice of methodology.

By now, it is clear that NAS suffers from a combinatorial explosion in its search space. One of the most common approaches to tackling this problem is to approximate the binary optimisation variables (i.e., edges in our case) with continuous counterparts. With such an approximation, traditional gradient-based optimisation techniques can be easily adopted. In fact, DARTS (Liu et al., 2019) utilises this strategy while attempting to acquire optimal neural architectures. Though successful in specific instances, DARTS and the likes suffer from two main drawbacks.

First, these algorithms are memory and computationally intensive ($\mathcal{O}(NK)$ with K being total number of operations between a pair of nodes and N the number of nodes) as they require loading all operation parameters into GPU memory. Due to these restrictions, DARTS only optimises over a small subset of 8 cells, which are then stacked together to form the deep network. Clearly, such an approximation is bound to be sub-optimal.

The second problem faced by gradient-based NAS algorithms is related to architecture testing, and, in fact, shared by almost all NAS algorithms. Precisely, evaluating an architecture amounts to a prediction on a validation set using the optimal set of network parameters. Learning these, unfortunately, is highly demanding since for an architecture \mathcal{Z}_t , one would like to compute $\mathcal{L}_t^{(\text{val})}(\mathcal{Z}_t, \mathbf{w}_t^*)$ where $\mathbf{w}_t^* = \arg \min_{\mathbf{w}} \mathcal{L}_t^{(\text{train})}(\mathbf{w}, \mathcal{Z}_t)$. DARTS, for instance, handles such inefficiencies using *weight sharing* that updates \mathbf{w}_t once per architecture, with the hope of tracking \mathbf{w}_t^* over learning rounds. Although this technique leads to significant speed up in computation, it is not clear how this approximation affects the validation loss function, or if it converges at all.

Next, we detail a novel methodology based on a combination of multi-agent and online learning to tackle the above two problems. Most notably, multi-agent learning scales our algorithm, reducing memory consumption by an order of magnitude from $\mathcal{O}(NK)$ to $\mathcal{O}(N)$, and online learning enables rigorous understanding of the effect of tracking \mathbf{w}_t^* over rounds.

3.1 Re-Formulation of Neural Architecture Search

Our contribution to NAS is unique in that it poses a novel formulation based on multi-agent-online-learning. Namely, we introduce a set of agents to control a small subset of operations. These sequentially interact with an environment receiving feedback to update their sampling strategy over associated operations. To address the memory consumption issue, in our method each agent sequentially samples different operations and learns in an online fashion based on the quality of each tested operation. Since each agent samples exactly one operation, this offers an improvement of the memory load over others by a factor equal to the number of available operations K . Moreover, due to

Algorithm 1 GENERAL FRAMEWORK: [steps with asterisks (*) are specified in section 4]

- 1: **Initialize:** $\pi_1^{(\mathcal{A}_i)}$ is uniform random over all $j \in \{1, \dots, N\}$. And random w_1 weights.
 - 2: **For** $t = 1, \dots, T$
 - 3: * Agent \mathcal{A}_i samples $\mathbf{a}_t^{(\mathcal{A}_i)} \sim \pi_t^{(\mathcal{A}_i)}(\mathbf{a}_t^{(\mathcal{A}_i)})$ for all $i \in \{1, \dots, N\}$, forming architecture \mathcal{Z}_t .
 - 4: Compute the loss $\mathcal{L}_t^{(\text{val})}(\mathbf{a}_t) = \mathcal{L}_t^{(\text{val})}(\mathcal{Z}_t, \mathbf{w}_t)$ on a batch of data.
 - 5: Update \mathbf{w}_{t+1} for all operation $\mathbf{a}_t^{(\mathcal{A}_i)}$ in \mathcal{Z}_t from \mathbf{w}_t using back-propagation on a batch data.
 - 6: * Update $\pi_{t+1}^{(\mathcal{A}_j)}$ for all $j \in \{1, \dots, N\}$ using $\mathcal{Z}_1, \dots, \mathcal{Z}_t$ and $\mathcal{L}_1^{(\text{val})}, \dots, \mathcal{L}_t^{(\text{val})}$.
 - 7: **Recommend** \mathcal{Z}_{T+1} , after round T , where $\mathbf{a}_{T+1}^{(\mathcal{A}_i)} \sim \pi_{T+1}^{(\mathcal{A}_i)}(\mathbf{a}_{T+1}^{(\mathcal{A}_i)})$ for all $i \in \{1, \dots, N\}$.
-

the 1:1 correspondence in memory consumption in search and augmentation phases, we are able to search directly on 20 cells without the need to repeat cells, as in DARTS.

To address the computational complexity problem we also use the weight sharing technique of DARTS. However, we try to handle in a more theoretically grounded way the effect of approximation of $\mathcal{L}_t^{(\text{val})}(\mathcal{Z}_t, \mathbf{w}_t^*)$ by $\mathcal{L}_t^{(\text{val})}(\mathcal{Z}_t, \mathbf{w}_t)$. Indeed, such an approximation can lead to arbitrary bad solutions due to the uncontrollable weight component. To analyse the learning problem with no stochastic assumptions on the process generating $\nu = \{\mathcal{L}_1, \dots, \mathcal{L}_T\}$ we adopt adversarial online learning framework that we detail next.

Neural Architecture Search as Multi-Agent Combinatorial Online Learning: In Section 2, we defined a NAS problem where one out of K operations needs to be recommended for each pair of nodes (i, j) in a DAG. In this section, we associate *each pair* of nodes with an *agent* that is in charge of exploring and locally quantifying the quality of these K operations and ultimately recommending one. However, the only feedback for each agent is the loss that is associated with a global architecture \mathcal{Z} that is the combination of all agents' choices.

We introduce N decision makers, $\mathcal{A}_1, \dots, \mathcal{A}_N$ (see Figure 1 and Algorithm 1). At training round t , each agent chooses an operation (e.g., convolution or pooling filter) according to its local action-distribution (or policy) $\mathbf{a}_t^{(\mathcal{A}_j)} \sim \pi_t^{(\mathcal{A}_j)}(\mathbf{a}_t^{(\mathcal{A}_j)})$, for all $j \in \{1, \dots, N\}$ with $\mathbf{a}_t^{(\mathcal{A}_j)} \in \{1, \dots, K\}$. These operations have corresponding operational weights \mathbf{w}_t that are learned in parallel. Altogether, these choices $\mathbf{a}_t = \mathbf{a}_t^{(\mathcal{A}_1)}, \dots, \mathbf{a}_t^{(\mathcal{A}_N)}$ define a sparse graph/architecture $\mathcal{Z}_t \equiv \mathbf{a}_t$ (see Section 2) for which a validation loss $\mathcal{L}_t^{(\text{val})}(\mathcal{Z}_t, \mathbf{w}_t)$ is computed and used by the agents to update their action selection rules. Ultimately after T tests, an architecture can be recommended by each agents $\mathbf{a}_{T+1}^{(\mathcal{A}_j)} \sim \pi_{T+1}^{(\mathcal{A}_j)}(\mathbf{a}_{T+1}^{(\mathcal{A}_j)})$, for all $j \in \{1, \dots, N\}$. These dynamics resemble bandit algorithms where the actions for an agent, \mathcal{A}_j are viewed as separate arms. This proposed MA framework leaves open the design of **1)** the sampling strategy $\pi^{(\mathcal{A}_j)}$ and **2)** how $\pi^{(\mathcal{A}_j)}$ is updated from the observed loss.

Given ν , minimise worst-case regret under any loss observation. We now introduce two notions of regret that motivates our proposed approaches. Given a policy π the *cumulative regret* $\mathcal{R}_{T,\pi}^*$ and the *simple regret* $r_{T,\pi}^*$ after T rounds and under the worst possible environment ν , are:

$$\mathcal{R}_{T,\pi}^* = \sup_{\nu} \mathbb{E} \sum_{t=1}^T \mathcal{L}_t(\mathbf{a}_t) - \min_{\mathbf{a}} \sum_{t=1}^T \mathcal{L}_t(\mathbf{a}), \quad r_{T,\pi}^* = \sup_{\nu} \mathbb{E} \sum_{t=1}^T \mathcal{L}_t(\mathbf{a}_{T+1}) - \min_{\mathbf{a}} \sum_{t=1}^T \mathcal{L}_t(\mathbf{a}) \quad (3)$$

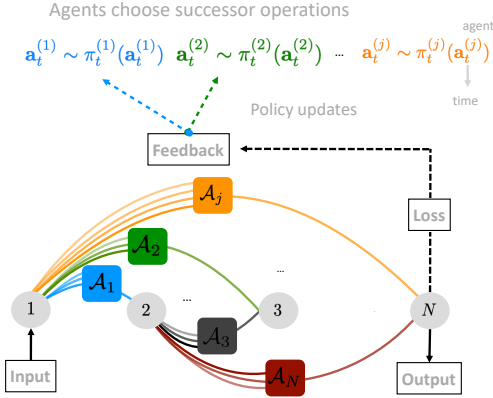


Figure 1: Multi-agent NAS with single cell NN. Between each pair of nodes, an agent \mathcal{A}_i selects action $a^{(i)}$ according to $\pi^{(i)}$. Feedback from the validation loss is used to update the policy.

where the expectation is taken over both the losses and policy distributions and $\mathbf{a} = \{\mathbf{a}^{(A_j)}\}_{j=1}^N$ denotes a joint action profile. While considering the simple regret leads to minimising directly the optimisation loss of the recommended architecture a_{T+1} , minimising the cumulative regret adds the extra requirement of having to sample, at any time t , architectures with close-to-optimal losses. We discuss in the appendix E how this requirement could improve in practice the tracking of w_t^* by w_t .

Combinatorial explosion and coordination of agents through credit assignment: Our problem introduces multiple agents in need of co-ordination for successful behaviour, and losses are intricate functions of each agent choices due to our focus on deep neural networks. Moreover, when defined naively, our problem suffer an exponential explosion in the total number of possible architectures \mathcal{Z} that is equal to K^N . We remedy the above problems by introducing approximate credit assignments between agents that quantifies the effect of actions chosen with respect to the overall validation loss. In turns this allows the agents to coordinate implicitly and remedy the combinatorial explosion.

4 Solution Methods

This section elaborates our solution methods for NAS when considering adversarial losses. We propose two *credit assignment techniques* in Section 4.1 that specify the update rule in line 6 of Algorithm 1. The first approximates the validation losses as linear combinations of edge weights, while the second directly handles the non-linear loss. We propose two sampling techniques in Section 4.2 that specify line 3 of Algorithm 1, one minimising the cumulative regret and one targeting the simple regret.

4.1 Decomposition of the Loss: Approximating Credit-Assignment

We address the combinatorial explosion of architectures by considering approximate credit-assignment that allows for scalability as each agent searches its local action space – typically small and finite – for optimal action-selection rules. In multi-agent learning, coordination can be achieved either implicitly or explicitly. Centralised critics, for example, advocate explicit coordination by learning the value of complex coordinated actions across all agents (Rashid et al., 2018). These algorithms are not scalable as they assume central information, making them inapplicable to neural search problems. In this paper, we argue for an implicit approach, where coordination is achieved through a joint (depending on all actions from all agents) loss function. Both credit assignment methods below learn for each operation k belonging to an agent \mathcal{A}_i a quantity $\tilde{\mathbf{B}}_t^{(A_i)}[k]$ (similar to the α from Section 2) that quantifies the contribution of the operation to the observed losses.

Linear Decomposition Clearly, seeking a closed form analytical solution to understanding the effect of an operation on the resulting overall loss is challenging. As such, we follow a simplified approximation scheme, shown effective in experiments, see Section 5, to assign credit to each of the agents’ action choices. Precisely, we attempt to approximate edge-importance (or edge-weight) through a linear combination of the architecture’s edges (i.e., agents’ actions) as, at each time t :

$$\mathcal{L}_t^{(\text{val})} = \beta_t^\top \mathbf{Z}_t$$

where $\mathbf{Z}_t \in \{0, 1\}^{KN}$ is a vectorised version of the architecture \mathcal{Z}_t containing all action choices and $\beta_t \in \mathbb{R}^{KN}$ is an arbitrary, potentially adversarially chosen sequence of vectors. Having collected a set of validation losses and architectures over varying rounds, we can regress for β_1, \dots, β_t either using gradient-descent or by applying the least-square equations, having

$$\text{Update: } \tilde{\mathbf{B}}_t = (\mathbf{Z}\mathbf{Z}^\top)^\dagger \mathbf{Z}\mathbf{L},$$

where \mathbf{A}^\dagger denotes the pseudo-inverse of \mathbf{A} , $\mathbf{Z} = [\mathbf{Z}_1, \mathbf{Z}_2, \dots, \mathbf{Z}_t]$ is a matrix collecting all architectures seen so-far, and $\mathbf{L} = [\mathcal{L}_1^{(\text{val})}, \mathcal{L}_2^{(\text{val})}, \dots, \mathcal{L}_t^{(\text{val})}]^\top$ is a vector of validation losses.

Though simple, the solution gives an efficient way for agents to update their corresponding action-selection rules which they implicitly coordinate. Indeed in Appendix C, we demonstrate that the worst-case regret \mathcal{R}_T^* (3) can actually be decomposed into an agent-specific form $\mathcal{R}_T^{(A_i)}(\pi^{(A_i)}, \nu^{(A_i)})$ defined in the appendix: $\mathcal{R}_T^* = \sup_\nu \mathcal{R}_T(\pi, \nu) \iff \sup_{\nu^{(A_i)}} \mathcal{R}_T^{(A_i)}(\pi^{(A_i)}, \nu^{(A_i)})$, $i = 1, \dots, N$. This decomposition allows us to significantly reduce the search space and apply upcoming sampling techniques for each agent \mathcal{A}_i in a completely parallel fashion.

Coordinated Descent for Non-Linear Losses As the linear approximation is likely to be crude, an alternative is to make no assumption on the loss function and have each agent directly associate the quality of their action with the loss $\mathcal{L}_t^{(\text{val})}(\mathbf{a}_t^{(\mathcal{A}_1)}, \dots, \mathbf{a}_t^{(\mathcal{A}_N)})$. This results in obtaining all the agents performing a coordinated descent approach to the problem. Each agent updates its $\tilde{\mathbf{B}}_t^{(\mathcal{A}_i)}[k]$ as

$$\text{Update: } \tilde{\mathbf{B}}_t^{(\mathcal{A}_i)}[k] = \tilde{\mathbf{B}}_{t-1}^{(\mathcal{A}_i)}[k] + \mathcal{L}_t^{(\text{val})}(\mathbf{a}_t^{(\mathcal{A}_1)}, \dots, \mathbf{a}_t^{(\mathcal{A}_N)}) \mathbb{1}_{\mathbf{a}_t^{(\mathcal{A}_i)}=k} / \pi_t^{(\mathcal{A}_i)}[k].$$

4.2 Sampling techniques

We propose two methods minimising the *simple regret* $r_{T,\pi}^*$ or the *cumulative regret* $\mathcal{R}_{T,\pi}^*$, (3).

Zipf Exploration for $r_{T,\pi}^*$: \mathcal{A}_i samples an operation k proportionally to the inverse of its estimated rank $\widetilde{\langle k \rangle}_t^{(\mathcal{A}_i)}$, where $\widetilde{\langle k \rangle}_t^{(\mathcal{A}_i)}$ is computed by sorting the operations of agent \mathcal{A}_i w.r.t $\tilde{\mathbf{B}}_t^{(\mathcal{A}_i)}[k]$, as

$$\text{Sampling policy: } \pi_{t+1}^{(\mathcal{A}_i)}[k] = 1 / \widetilde{\langle k \rangle}_t^{(\mathcal{A}_i)} \overline{\log K} \quad \text{where } \overline{\log K} = 1 + 1/2 + \dots + 1/K.$$

Zipf explores efficiently as, up to log factors, for $1 \leq m \leq K$, the m estimated best operations are picked uniformly ignoring the remaining $K - m$ operations: All operations are explored almost as in uniform exploration while the estimated best is picked almost all the time. The Zipf law is anytime, parameter free and minimises optimally the simple regret in the vanilla multi-armed bandit when the losses can be either adversarial or stochastic (Abbasi-Yadkori et al., 2018).

Softmax Sampling for $\mathcal{R}_{T,\pi}^*$ Based on EXP3 (Auer et al., 2002), samples are from a softmax distribution (with temperature η) w.r.t. $\tilde{\mathbf{B}}_t^{(\mathcal{A}_i)}[k]$ and the aim is to always pull the best operation as

$$\text{Sampling policy: } \pi_{t+1}^{(\mathcal{A}_i)}[k] = \exp\left(\eta \tilde{\mathbf{B}}_t^{(\mathcal{A}_i)}[k]\right) / \sum_{j=1}^K \exp\left(\eta \tilde{\mathbf{B}}_t^{(\mathcal{A}_i)}[j]\right) \quad \text{for } k = 1, \dots, K.$$

4.3 Theoretical guarantees

We provide regret bounds for the combinations of the above sampling and credit assignment methods.

- **Linear+Softmax:** we recover the multitask bandit instance of the ComBand algorithm (Cesa-Bianchi and Lugosi, 2012, Section 5.1) where the authors prove $\mathcal{R}_T^* = \mathcal{O}(N\sqrt{TK \log K})$.
- **Linear+Zipf:** we prove for this new algorithm an exponentially decreasing simple regret $r_T^* = \mathcal{O}(e^{-T/H})$, where H is a measure of the complexity for discriminating sub-optimal solutions as $H = N(\min_{j \neq k_i^*, 1 \leq i \leq N} \mathbf{B}_T^{(\mathcal{A}_i)}[j] - \mathbf{B}_T^{(\mathcal{A}_i)}[k_i^*])$, where $k_i^* = \min_{1 \leq j \leq K} \mathbf{B}_T^{(\mathcal{A}_i)}[j]$ and $\mathbf{B}_T^{(\mathcal{A}_i)}[j] = \sum_{t=1}^T \beta_t^{(\mathcal{A}_i)}[j]$. We report the proof in Appendix D.1.
- **Coordinated descent+Softmax** runs EXP3 for each agent in parallel. If the regret of each agent is computed by considering the rest of the agent as fixed, then each agent has regret $\mathcal{O}(\sqrt{TK \log K})$ which sums over agents to $\mathcal{O}(N\sqrt{TK \log K})$ (see proof in Appendix D.2). A similar analysis can be performed Coordinated descent+Zipf by reusing the results in Abbasi-Yadkori et al. (2018).

5 Experiments Results

This section is divided into three parts. Firstly, we compare MANAS against existing NAS methods on the well established Cifar-10 dataset. Secondly, we evaluate our solution on ImageNet and finally, we compare MANAS, DARTS and random sampling on 3 new datasets.

We report the performance of two algorithms, MANAS and MANAS-LS, that correspond respectively to the combination Coordinated+Softmax and Linear+Zipf in Section 4. Linear+Softmax proved in preliminary experiments to be harder to tune and was thus excluded from further experiments².

²Descriptions of the datasets and details of the search are provided in the Appendix.

Table 1: Comparison with state-of-the-art image classifiers on Cifar-10

| Architecture | Test Error (%) | Params (M) | Search Cost (GPU days) | Search Method |
|--|----------------|------------|------------------------|---------------|
| DenseNet-BC (Huang et al., 2017) | 3.46 | 25.6 | | manual |
| NASNet-A (Zoph et al., 2018) | 2.65 | 3.3 | 1800 | RL |
| AmoebaNet-B (Real et al., 2018) | 2.55 | 2.8 | 3150 | evolution |
| Hierarchical Evo (Liu et al., 2018b) | 3.75 | 15.7 | 300 | evolution |
| PNAS (Liu et al., 2018a) | 3.41 | 3.2 | 225 | SMBO |
| ENAS (Pham et al., 2018) | 2.89 | 4.6 | 0.5 | RL |
| SNAS (Xie et al., 2019) | 2.85 | 2.8 | 1.5 | gradient |
| DARTS, 1st order (Liu et al., 2019) [†] | 3.00 | 3.3 | 1.5 | gradient |
| DARTS, 2nd order (Liu et al., 2019) [†] | 2.76 | 3.3 | 4 | gradient |
| Random + cutout (Liu et al., 2019) | 3.29 | 3.2 | — | — |
| MANAS (8 cells) [†] | 3.05 | 1.6 | 0.8 | MA |
| MANAS (20 cells) [†] | 2.63 | 3.4 | 2.8 | MA |
| MANAS-LS (20 cells) [†] | 2.52 | 3.4 | 4 | MA |

[†] Search cost is for 4 runs and test error is for the best result (for a fair comparison with other methods).

Table 2: Comparison with state-of-the-art image classifiers on ImageNet (mobile setting)

| Architecture | Test Error (%) | Params (M) | Search Cost (GPU days) | Search Method |
|---|----------------|------------|------------------------|---------------|
| Inception-v1 (Szegedy et al., 2017) | 30.2 | 6.6 | | manual |
| MobileNet (Howard et al., 2017) | 29.4 | 4.2 | | manual |
| ShuffleNet 2x (v2) (Zhang et al., 2018) | 26.3 | 5 | | manual |
| NASNet-A (Zoph et al., 2018) | 26.0 | 5.3 | 1800 | RL |
| AmoebaNet-C (Real et al., 2018) | 24.3 | 6.4 | 3150 | evolution |
| PNAS (Liu et al., 2018a) | 25.8 | 5.1 | 225 | SMBO |
| SNAS (Xie et al., 2019) | 27.3 | 4.3 | 1.5 | gradient |
| DARTS (Liu et al., 2019) | 26.7 | 4.7 | 4 | gradient |
| Random | 27.75 | 2.5 | — | — |
| MANAS (searched on Cifar-10) | 26.47 | 2.6 | 2.8 | MA |
| MANAS (searched on ImageNet) | 26.15 | 2.6 | 110 | MA |

Search Space. We follow the same convolutional search space defined by Liu et al. (2019). Since our method is memory efficient, we can find the final architecture without needing to stack *a posteriori* repeated cells, thus all of our cells are unique. For a fair comparison, we used 20 cells on Cifar-10 (Krizhevsky, 2009) and 14 cells for ImageNet (Deng et al., 2009). Experiments on Sport-8 (Li and Fei-Fei, 2007), Caltech101 (Fei-Fei et al., 2007) and MIT67 (Quattoni and Torralba, 2009) in §5 use 8 and 14 cells.

Search Protocol. For datasets other than ImageNet, we use 500 epochs during the search phase for architectures with 20 cells, 400 epochs for 14 cells, and 50 epochs for 8 cells. All other meta-parameters such as learning rate decay, batch size, etc., are as in Liu et al. (2019). For ImageNet, we use 14 cells and 100 epochs during search. In our experiments on the three new datasets we rerun the DARTS code to optimise an 8 cell architecture; for 14 cells we simply stacked the best cells for the appropriate number of times.

Evaluation on Cifar-10. To evaluate our NAS algorithm, we follow DARTS’s protocol: we run MANAS 4 times with different random seeds and pick the best architecture based on its validation performance. We then randomly reinitialize the weights and train from scratch for 600 epochs. During the search phase we use half of the training set as validation.

Results. Both MANAS implementations perform well on this dataset (Table 1). Our algorithm is designed to perform comparably to Liu et al. (2019) but with an order of magnitude less memory:

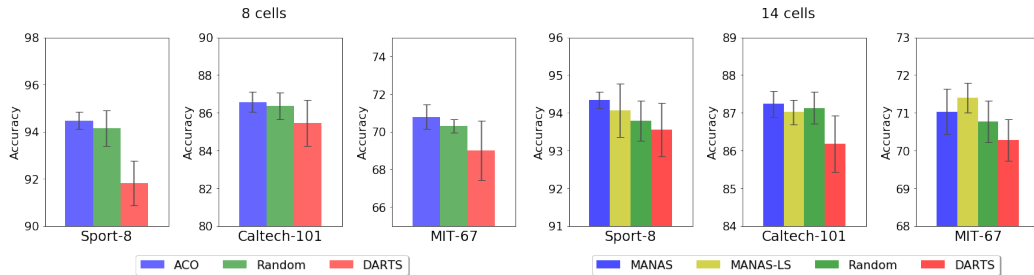


Figure 2: Comparing MANAS, random sampling and DARTS (Liu et al., 2019) on 8 and 14 cells. Average results of 8 runs. Note that DARTS was only optimised for 8 cells due to memory constraints.

why is it then that we actually have higher accuracy? The reason is that DARTS is forced to search for an 8 cell architecture and subsequently stack the same cells 20 times; MANAS, on the other hand, can directly search on the final number of cells leading to better results. We also report our results when using only 8 cells: even though the network is much smaller, it still performs very competitively. In our third sets of experiments we will explore this in more depth. Cai et al. (2019) is another method designed as an efficient alternative to DARTS; unfortunately the authors decided to a) use a different search space (PyramidNet backbone; Han et al. (2017)) and b) offer no comparison to random sampling in the given search space. For these reasons we feel a numerical comparison to be unfair. Furthermore our algorithm uses half the GPU memory (they sample 2 paths at a time) and does not require the reward to be differentiable.

Evaluation on ImageNet. To evaluate the results on ImageNet we train the final architecture for 250 epochs. We report the result of the best architecture out of 4, as chosen on the validation set for a fair comparison with competing methods. Because search and augmentation are very expensive we use only MANAS and not MANAS-LS, as the former is computationally cheaper and performs slightly better on average (further experiments presented below).

Results. We provide results for networks searched both on Cifar-10 and directly on ImageNet, which is made possible by the computational efficiency of MANAS (Table 2). When compared to SNAS and DARTS—currently the most efficient methods, using the same search space, available—MANAS achieves state-of-the-art results both with architectures searched directly on ImageNet (0.85 p.p. improvement) and also with architectures transferred from Cifar-10 (0.55 p.p. improvement).

Evaluation on three new datasets. The idea behind NAS is that of finding the optimal architecture, given *any* sets of data and labels. Limiting the evaluation of current methods to Cifar-10 and ImageNet could potentially lead to algorithmic overfitting. Indeed, recent results suggest that the search space was engineered in a way that makes it very hard to find a bad architecture (Li and Talwalkar, 2019; Sciuto et al., 2019). To mitigate this, we propose testing NAS algorithms on 3 datasets (composed of regular sized images) that were never before used in this setting, but have been historically used in the CV field: Sport-8, Caltech-101 and MIT-67, described briefly in the Appendix. For these set of experiments we run the algorithm 8 times and report mean and std. We perform this both for 8 and 14 cells; we do the same with DARTS (which, due to memory constraints can only be run for 8 cells). For our random baseline we sample uniformly 8 architectures from the search space. Each proposed architecture is then trained from scratch for 600 epochs as in the previous section.

Results. For these experiments can be found in Figure 2. MANAS manages to outperform the random baseline and significantly outperform DARTS, especially on 14 cells. It can be clearly seen from our experiments, that the optimal cell architecture for 8 cells is *not* the optimal one for 14 cells.

Discussion on Random Search. Clearly, in specific settings, random sampling performs very competitively. On one hand, since the search space is very large (between 8^{112} and 8^{280} architectures exist in the DARTS experiments; Liu et al., 2019), finding the global optimum is practically impossible. Why is it then that the randomly sampled architectures are able to deliver nearly state-of-the-art results? Previous experiments (Sciuto et al., 2019; Li and Talwalkar, 2019) together with the results presented here seem to indicate that the available operations and meta-structure have been carefully chosen and, as a consequence, most architectures in this space generate meaningful results. This

suggests that human effort has simply transitioned from finding a good architecture to finding a good search space – a problem that needs careful consideration in future work.

6 Conclusions

We presented MANAS, a theoretically grounded multi-agent online learning framework for NAS. We then proposed two extremely lightweight implementations that, within the same search space, outperform state-of-the-art while reducing memory consumption by an order of magnitude compared to Liu et al. (2019). We provide vanishing regret proofs for our algorithms. Furthermore, we evaluate MANAS on 3 new datasets, empirically showing its effectiveness in a variety of settings.

In order to further improve MANAS, future research will focus on why random search presents a strong baseline. Likely, as noted by previous work Li and Talwalkar (2019); Sciuto et al. (2019), weight sharing can be one key contributor to this fact – a hypothesis we aim to validate in the future.

References

- Yasin Abbasi-Yadkori, Peter Bartlett, Victor Gabillon, Alan Malek, and Michal Valko. Best of both worlds: Stochastic & adversarial best-arm identification. In *Conference on Learning Theory (COLT)*, 2018.
- Peter Auer, Nicolo Cesa-Bianchi, Yoav Freund, and Robert E Schapire. The nonstochastic multiarmed bandit problem. *SIAM journal on computing*, 32(1):48–77, 2002.
- Sébastien Bubeck, Nicolo Cesa-Bianchi, et al. Regret analysis of stochastic and nonstochastic multi-armed bandit problems. *Foundations and Trends® in Machine Learning*, 5(1):1–122, 2012.
- Han Cai, Ligeng Zhu, and Song Han. ProxylessNAS: Direct neural architecture search on target task and hardware. In *International Conference on Learning Representations (ICLR)*, 2019.
- Nicolo Cesa-Bianchi and Gábor Lugosi. Combinatorial bandits. *Journal of Computer and System Sciences*, 78(5):1404–1422, 2012.
- Alexis Conneau, Holger Schwenk, Loïc Barrault, and Yann Lecun. Very deep convolutional networks for text classification. In *European Chapter of the Association for Computational Linguistics: Volume 1, Long Papers*, pages 1107–1116, 2017.
- Jia Deng, Wei Dong, Richard Socher, Li-Jia Li, Kai Li, and Li Fei-Fei. ImageNet: A large-scale hierarchical image database. In *Computer Vision and Pattern Recognition (CVPR)*, pages 248–255, 2009.
- Li Fei-Fei, Rob Fergus, and Pietro Perona. Learning generative visual models from few training examples: An incremental bayesian approach tested on 101 object categories. *Computer Vision and Image Understanding*, 106(1):59–70, 2007.
- David A. Freedman. On tail probabilities for martingales. *The Annals of Probability*, pages 100–118, 1975.
- Dongyoon Han, Jiwhan Kim, and Junmo Kim. Deep pyramidal residual networks. In *Computer Vision and Pattern Recognition (CVPR)*, pages 5927–5935, 2017.
- Kaiming He, Xiangyu Zhang, Shaoqing Ren, and Jian Sun. Deep residual learning for image recognition. In *Computer Vision and Pattern Recognition (CVPR)*, pages 770–778, 2016.
- Andrew G Howard, Menglong Zhu, Bo Chen, Dmitry Kalenichenko, Weijun Wang, Tobias Weyand, Marco Andreetto, and Hartwig Adam. MobileNets: Efficient convolutional neural networks for mobile vision applications. *arXiv:1704.04861*, 2017.
- Gao Huang, Zhuang Liu, Laurens Van Der Maaten, and Kilian Q Weinberger. Densely connected convolutional networks. In *Computer Vision and Pattern Recognition (CVPR)*, pages 4700–4708, 2017.

- ByungSoo Ko. Imagenet classification leaderboard. <https://kobiso.github.io/Computer-Vision-Leaderboard/imagenet>, 2019.
- Alex Krizhevsky. Learning multiple layers of features from tiny images. Technical report, University of Toronto, 2009.
- Li-Jia Li and Li Fei-Fei. What, where and who? classifying events by scene and object recognition. In *International Conference on Computer Vision (ICCV)*, pages 1–8, 2007.
- Liam Li and Ameet Talwalkar. Random search and reproducibility for neural architecture search. *arXiv:1902.07638*, 2019.
- Chenxi Liu, Barret Zoph, Maxim Neumann, Jonathon Shlens, Wei Hua, Li-Jia Li, Li Fei-Fei, Alan Yuille, Jonathan Huang, and Kevin Murphy. Progressive neural architecture search. In *European Conference on Computer Vision (ECCV)*, pages 19–34, 2018a.
- Hanxiao Liu, Karen Simonyan, Oriol Vinyals, Chrisantha Fernando, and Koray Kavukcuoglu. Hierarchical representations for efficient architecture search. In *International Conference on Learning Representations (ICLR)*, 2018b.
- Hanxiao Liu, Karen Simonyan, and Yiming Yang. DARTS: Differentiable architecture search. In *International Conference on Learning Representations (ICLR)*, 2019.
- Stephen Merity, Nitish Shirish Keskar, and Richard Socher. Regularizing and optimizing LSTM language models. In *International Conference on Learning Representations (ICLR)*, 2018.
- Hieu Pham, Melody Guan, Barret Zoph, Quoc Le, and Jeff Dean. Efficient neural architecture search via parameter sharing. In *International Conference on Machine Learning (ICML)*, pages 4092–4101, 2018.
- Ariadna Quattoni and Antonio Torralba. Recognizing indoor scenes. In *Computer Vision and Pattern Recognition (CVPR)*, pages 413–420, 2009.
- Tabish Rashid, Mikayel Samvelyan, Christian Schroeder Witt, Gregory Farquhar, Jakob Foerster, and Shimon Whiteson. QMIX: Monotonic value function factorisation for deep multi-agent reinforcement learning. In *International Conference on Machine Learning (ICML)*, pages 4292–4301, 2018.
- Esteban Real, Sherry Moore, Andrew Selle, Saurabh Saxena, Yutaka Leon Suematsu, Jie Tan, Quoc V Le, and Alexey Kurakin. Large-scale evolution of image classifiers. In *International Conference on Machine Learning (ICML)*, pages 2902–2911, 2017.
- Esteban Real, Alok Aggarwal, Yanping Huang, and Quoc V Le. Regularized evolution for image classifier architecture search. *arXiv:1802.01548*, 2018.
- Christian Sciuto, Kaicheng Yu, Martin Jaggi, Claudiu Musat, and Mathieu Salzmann. Evaluating the search phase of neural architecture search. *arXiv:1902.08142*, 2019.
- Christian Szegedy, Sergey Ioffe, Vincent Vanhoucke, and Alexander A Alemi. Inception-v4, Inception-ResNet and the impact of residual connections on learning. In *AAAI Conference on Artificial Intelligence*, 2017.
- Sirui Xie, Hehui Zheng, Chunxiao Liu, and Liang Lin. SNAS: Stochastic neural architecture search. In *International Conference on Learning Representations (ICLR)*, 2019.
- Xiangyu Zhang, Xinyu Zhou, Mengxiao Lin, and Jian Sun. ShuffleNet: An extremely efficient convolutional neural network for mobile devices. In *Conference on Computer Vision and Pattern Recognition (CVPR)*, pages 6848–6856, 2018.
- Barret Zoph and Quoc Le. Neural architecture search with reinforcement learning. In *International Conference on Learning Representations (ICLR)*, 2017.
- Barret Zoph, Vijay Vasudevan, Jonathon Shlens, and Quoc V Le. Learning transferable architectures for scalable image recognition. In *Computer Vision and Pattern Recognition (CVPR)*, pages 8697–8710, 2018.

A Datasets

Cifar-10. The CIFAR-10 dataset (Krizhevsky, 2009) is a dataset of 10 classes and consists of 50,000 training images and 10,000 test images of size 32×32 . We use standard data pre-processing and augmentation techniques, i.e. subtracting the channel mean and dividing the channel standard deviation; centrally padding the training images to 40×40 and randomly cropping them back to 32×32 ; and randomly flipping them horizontally.

ImageNet. The ImageNet dataset (Deng et al., 2009) is a dataset of 1000 classes and consists of 1,281,167 training images and 50,000 test images of different sizes. We use standard data pre-processing and augmentation techniques, i.e. subtracting the channel mean and dividing the channel standard deviation, cropping the training images to random size and aspect ratio, resizing them to 224×224 , and randomly changing their brightness, contrast, and saturation, while resizing test images to 256×256 and cropping them at the center.

Sport-8. This is an action recognition dataset containing 8 sport event categories and a total of 1579 images (Li and Fei-Fei, 2007). The tiny size of this dataset stresses the generalization capabilities of any NAS method applied to it.

Caltech-101. This dataset contains 101 categories, each with 40 to 800 images of size roughly 300×200 (Fei-Fei et al., 2007).

MIT-67. This is a dataset of 67 classes representing different indoor scenes and consists of 15,620 images of different sizes (Quattoni and Torralba, 2009).

In experiments on Sport-8, Caltech-101 and MIT-67, we split each dataset into a training set containing 80% of the data and a test set containing 20% of the data. For each of them, we use the same data pre-processing techniques as for ImageNet.

B Implementation details

B.1 Methods

MANAS. Our code is based on a modified variant of Liu et al. (2019). To set the temperature and gamma, we used as starting estimates the values suggested by Bubeck et al. (2012): $t = \frac{1}{\eta}$ with $\eta = 0.95 \frac{\sqrt{\ln(K)}}{nK}$ (K number of actions, n number of architectures seen in the whole training). $\gamma = 1.05 \frac{K \ln(K)}{n}$. We then tuned them to increase validation accuracy during the search.

MANAS-LS. For our Least-Squares solution, we alternate between one epoch of training (in which all β are frozen and the ω are updated) and one or more epochs in which we build the Z matrix from Section 4 (in which both β and ω are frozen). The exact number of iterations we perform in this latter step is dependant on the size of both the dataset and the searched architecture: our goal is simply to have a number of rows greater than the number of columns for Z . We then solve $\tilde{\mathbf{B}}_t = (\mathbf{Z}\mathbf{Z}^T)^\dagger \mathbf{Z}\mathbf{L}$, and repeat the whole procedure until the end of training. This method requires no additional meta-parameters.

B.2 Computational resources

ImageNet experiments were performed on multi-GPU machines loaded with $8 \times$ Nvidia Tesla V100 16GB GPUs (used in parallel). All other experiments were performed on single-GPU machines loaded with $1 \times$ GeForce GTX 1080 8GB GPU.

C Factorizing the Regret

Factorizing the Regret: Let us firstly formulate the multi-agent combinatorial online learning in a more formal way. Recall, at each round, agent \mathcal{A}_i samples an action from a fixed discrete collection $\{\mathbf{a}_j^{(\mathcal{A}_i)}\}_{j=1}^K$. Therefore, after each agent makes a choice of its action at round t , the resulting network architecture \mathcal{Z}_t is described by joint action profile $\vec{\mathbf{a}}_t = [\mathbf{a}_{j_1}^{(\mathcal{A}_1),[t]}, \dots, \mathbf{a}_{j_N}^{(\mathcal{A}_N),[t]}]$

and thus, we will use \mathcal{Z}_t and \vec{a}_t interchangeably. Due to the discrete nature of the joint action space, the validation loss vector at round t is given by $\vec{\mathcal{L}}_t^{(\text{val})} = \left(\mathcal{L}_t^{(\text{val})}(\mathcal{Z}_t^{(1)}), \dots, \mathcal{L}_t^{(\text{val})}(\mathcal{Z}_t^{(K^N)}) \right)$ and for the environment one can write $\nu = \left(\vec{\mathcal{L}}_1^{(\text{val})}, \dots, \vec{\mathcal{L}}_T^{(\text{val})} \right)$. The interconnection between joint policy π and an environment ν works in a sequential manner as follows: at round t , the architecture $\mathcal{Z}_t \sim \pi_t(\cdot | \mathcal{Z}_1, \mathcal{L}_1^{(\text{val})}, \dots, \mathcal{Z}_{t-1}, \mathcal{L}_{t-1}^{(\text{val})})$ is sampled and validation loss $\mathcal{L}_t^{(\text{val})} = \mathcal{L}_t^{(\text{val})}(\mathcal{Z}_t)$ is observed³. As we mentioned previously, assuming linear contribution of each individual actions to the validating loss, one goal is to find a policy π that keeps the regret:

$$\mathcal{R}_T(\pi, \nu) = \mathbb{E} \left[\sum_{t=1}^T \beta_t^\top \mathbf{Z}_t - \min_{\mathbf{Z} \in \mathcal{F}} \left[\sum_{t=1}^T \beta_t^\top \mathbf{Z} \right] \right] \quad (4)$$

small with respect to all possible forms of environment ν . We reason here with the cumulative regret the reasoning applies as well to the simple regret. Here, $\beta_t \in \mathbb{R}_+^{KN}$ is a contribution vector of all actions and \mathbf{Z}_t is binary representation of architecture \mathcal{Z}_t and $\mathcal{F} \subset [0, 1]^{KN}$ is set of all feasible architectures⁴. In other words, the quality of the policy is defined with respect to worst-case regret:

$$\mathcal{R}_T^* = \sup_{\nu} \mathcal{R}_T(\pi, \nu) \quad (5)$$

Notice, that linear decomposition of the validation loss allows to rewrite the total regret (4) as a sum of agent-specific regret expressions $\mathcal{R}_T^{(\mathcal{A}_i)}(\pi^{(\mathcal{A}_i)}, \nu^{(\mathcal{A}_i)})$ for $i = 1, \dots, N$:

$$\begin{aligned} \mathcal{R}_T(\pi, \nu) &= \mathbb{E} \left[\sum_{t=1}^T \left(\sum_{i=1}^N \beta_t^{(\mathcal{A}_i), \top} \mathbf{Z}_t^{(\mathcal{A}_i)} - \sum_{i=1}^N \min_{\mathbf{Z}^{(\mathcal{A}_i)} \in \mathcal{B}_{\|\cdot\|_0, 1}^{(K)}(\mathbf{0})} \left[\sum_{t=1}^T \beta_t^{(\mathcal{A}_i), \top} \mathbf{Z}^{(\mathcal{A}_i)} \right] \right) \right] \\ &= \sum_{i=1}^N \mathbb{E} \left[\sum_{t=1}^T \beta_t^{(\mathcal{A}_i), \top} \mathbf{Z}_t^{(\mathcal{A}_i)} - \min_{\mathbf{Z}^{(\mathcal{A}_i)} \in \mathcal{B}_{\|\cdot\|_0, 1}^{(K)}(\mathbf{0})} \left[\sum_{t=1}^T \beta_t^{(\mathcal{A}_i), \top} \mathbf{Z}^{(\mathcal{A}_i)} \right] \right] \\ &= \sum_{i=1}^N \mathcal{R}_T^{(\mathcal{A}_i)}(\pi^{(\mathcal{A}_i)}, \nu^{(\mathcal{A}_i)}) \end{aligned}$$

where $\beta_t = \left[\beta_t^{\mathcal{A}_1, \top}, \dots, \beta_t^{\mathcal{A}_N, \top} \right]^\top$ and $\mathbf{Z}_t = \left[\mathbf{Z}_t^{(\mathcal{A}_1), \top}, \dots, \mathbf{Z}_t^{(\mathcal{A}_N), \top} \right]^\top$, $\mathbf{Z} = \left[\mathbf{Z}^{(\mathcal{A}_1), \top}, \dots, \mathbf{Z}^{(\mathcal{A}_N), \top} \right]^\top$ are decomposition of the corresponding vectors on agent-specific parts, joint policy $\pi(\cdot) = \prod_{i=1}^N \pi^{(\mathcal{A}_i)}(\cdot)$, and joint environment $\nu = \prod_{i=1}^N \nu^{(\mathcal{A}_i)}$, and $\mathcal{B}_{\|\cdot\|_0, 1}^{(K)}(\mathbf{0})$ is unit ball with respect to $\|\cdot\|_0$ norm centered at $\mathbf{0}$ in $[0, 1]^K$. Moreover, the worst-case regret (5) also can be decomposed into agent-specific form:

$$\mathcal{R}_T^* = \sup_{\nu} \mathcal{R}_T(\pi, \nu) \iff \sup_{\nu^{(\mathcal{A}_i)}} \mathcal{R}_T^{(\mathcal{A}_i)}(\pi^{(\mathcal{A}_i)}, \nu^{(\mathcal{A}_i)}), \quad i = 1, \dots, N.$$

This decomposition allows us to significantly reduce the search space and apply the two following algorithms for each agent \mathcal{A}_i in a completely parallel fashion.

D Theoretical Guarantees

D.1 Combining Linear decomposition and Zipf Sampling

First, we need to be more specific on the way to obtain the estimates $\tilde{\beta}_t^{(\mathcal{A}_i)}[k]$.

In order to obtain theoretical guaranties we considered the least-square estimates as in [Cesa-Bianchi and Lugosi \(2012\)](#) as

³Please notice, the observed reward is actually a random variable

⁴We assume that architecture is feasible if and only if each agent chooses exactly one action.

$$\tilde{\beta}_t = \mathcal{L}_t^{(\text{val})} \mathbf{P}^\dagger \mathbf{Z}_t \text{ where } \mathbf{P} = \mathbb{E} [\mathbf{Z}\mathbf{Z}^T] \text{ with } \mathbf{Z} \text{ has law } \pi_t(\cdot) = \prod_{i=1}^N \pi_t^{(\mathcal{A}_i)}(\cdot) \quad (6)$$

Our analysis is under the assumption that each $\beta_t \in \mathbb{R}^{KN}$ belongs to the linear space spanned by the space of sparse architecture \mathcal{Z} . This is not a strong assumption as the only condition on a sparse architecture comes with the sole restriction that one operation for each agent is active.

Theorem 1. *Let us consider neural architecture search problem in a multi-agent combinatorial online learning form with N agents such that each agent has K actions. Then after T rounds, Linear + Zipf achieves joint policy $\{\pi_i\}_{i=1}^T$ with expected simple regret (Equation 3) bounded by $\mathcal{O}(e^{-T/H})$ in any adversarial environment with complexity bounded by $H = N(\min_{j \neq k_i^*, i \in \{1, \dots, N\}} \mathbf{B}_T^{(\mathcal{A}_i)}[j] - \mathbf{B}_T^{(\mathcal{A}_i)}[k_i^*])$, where $k_i^* = \min_{j \in \{1, \dots, K\}} \mathbf{B}_T^{(\mathcal{A}_i)}[j]$.*

Proof. In Equation 6 we use the same constructions of estimates $\tilde{\beta}_t$ as in ComBand. Using Corollary 14 in Cesa-Bianchi and Lugosi (2012) we then have that $\tilde{\mathbf{B}}_t$ is an unbiased estimates of \mathbf{B}_t .

Given the adversary losses, the random variables $\tilde{\beta}_t$ can be dependent of each other and $t \in [T]$ as π_t depends on previous observations at previous rounds. Therefore, we use the Azuma inequality for martingale differences by Freedman (1975).

Without loss of generality we assume that the loss $\mathcal{L}_t^{(\text{val})}$ are bounded such that $\mathcal{L}_t^{(\text{val})} \in [0, 1]$ for all t . Therefore we can bound the simple regret of each agent by the probability of misidentifying of the best operation $P(k_i^* \neq a_{T+1}^{A_i})$.

We consider a fixed adversary of complexity bounded by H . For simplicity, and without loss of generality, we order the operations from such that $\mathbf{B}_T^{(\mathcal{A}_i)}[1] < \mathbf{B}_T^{(\mathcal{A}_i)}[2] \leq \dots \leq \mathbf{B}_T^{(\mathcal{A}_i)}[K]$ for all agents.

We denote for $k > 1$, $\Delta_k = \mathbf{B}_T^{(\mathcal{A}_i)}[k] - \mathbf{B}_T^{(\mathcal{A}_i)}[k_i^*]$ and $\Delta_1 = \Delta_2$.

We also have λ_{\min} as the smallest nonzero eigenvalue of \mathbf{M} where \mathbf{M} is $\mathbf{M} = E[\mathbf{Z}\mathbf{Z}^T]$ where \mathbf{Z} is a random vector representing a sparse architecture distributed according to the uniform distribution.

$$\begin{aligned} P(k_i^* \neq a_{T+1}^{A_i}) &= P\left(\exists k \in \{1, \dots, K\} : \tilde{\mathbf{B}}_T^{(\mathcal{A}_i)}[1] \geq \tilde{\mathbf{B}}_T^{(\mathcal{A}_i)}[k]\right) \\ &\leq P\left(\exists k \in \{1, \dots, K\} : \mathbf{B}_T^{(\mathcal{A}_i)}[k] - \tilde{\mathbf{B}}_T^{(\mathcal{A}_i)}[k] \geq \frac{T\Delta_k}{2} \text{ or } \tilde{\mathbf{B}}_T^{(\mathcal{A}_i)}[1] - \mathbf{B}_T^{(\mathcal{A}_i)}[1] \geq \frac{T\Delta_1}{2}\right) \\ &\leq P\left(\tilde{\mathbf{B}}_T^{(\mathcal{A}_i)}[1] - \mathbf{B}_T^{(\mathcal{A}_i)}[1] \geq \frac{T\Delta_1}{2}\right) + \sum_{k=2}^K P\left(\mathbf{B}_T^{(\mathcal{A}_i)}[k] - \tilde{\mathbf{B}}_T^{(\mathcal{A}_i)}[k] \geq \frac{T\Delta_k}{2}\right) \\ &\stackrel{\text{(a)}}{\leq} \sum_{k=1}^K \exp\left(-\frac{(\Delta_k)^2 T}{2N \log(K) / \lambda_{\min}}\right) \\ &\leq K \exp\left(-\frac{(\Delta_1)^2 T}{2N \log(K) / \lambda_{\min}}\right), \end{aligned}$$

where (a) is using Azuma's inequality for martingales applied to the sum of the random variables with mean zero that are $\tilde{\beta}_{k,t} - \beta_{k,t}$ for which we have the following bounds on the range. The range of $\tilde{\beta}_{k,t}$ is $[0, N \log(K) / \lambda_{\min}]$. Indeed our sampling policy is uniform with probability $1/\log(K)$ therefore one can bound $\tilde{\beta}_{k,t}$ as in (Cesa-Bianchi and Lugosi, 2012, Theorem 1) Therefore we have $|\tilde{\beta}_{k,t} - \beta_{k,t}| \leq N \log(K) / \lambda_{\min}$.

We recover the result with a union bound on all agents. \square

D.2 Combining Coordinated Decomposition and Softmax Sampling

We consider a simplified notion of regret that is a regret per agent where each agent is considering the rest of the agents as part of the adversarial environment. Let us fix our new objective as to minimise

$$\sum_{i=1}^N \mathcal{R}_T^{*,i}(\pi^{(\mathcal{A}_i)}) = \sum_{i=1}^N \sup_{\mathbf{a}_{-i}, \nu} \mathbb{E} \left[\sum_{t=1}^T \mathcal{L}_t^{(\text{val})}(\mathbf{a}_t^{(\mathcal{A}_i)}, \mathbf{a}_{-i}) - \min_{\mathbf{a} \in \{1, \dots, K\}} \left[\sum_{t=1}^T \mathcal{L}_t^{(\text{val})}(\mathbf{a}, \mathbf{a}_{-i}) \right] \right],$$

where \mathbf{a}_{-i} is a fixed set of actions played by all agents to the exception of agent \mathcal{A}_i for the T rounds of the game and ν contains all the losses as $\nu = \{\mathcal{L}_t^{(\text{val})}(\mathbf{a})\}_{t \in \{1, \dots, T\}, \mathbf{a} \in \{1, \dots, K^N\}}$.

We then can prove the following bound for that new notion of regret.

Theorem 2. *Let us consider neural architecture search problem in a multi-agent combinatorial online learning form with N agents such that each agent has K actions. Then after T rounds, combining Coordinated + Softmax achieves joint policy $\{\pi_t\}_{t=1}^T$ with expected cumulative regret bounded by $\mathcal{O}(N\sqrt{TK \log K})$.*

Proof. First we look at the problem for each given agent \mathcal{A}_i and we define and look at

$$\mathcal{R}_T^{*,i}(\pi^{(\mathcal{A}_i)}, \mathbf{a}_{-i}) = \sup_{\nu} \mathbb{E} \left[\sum_{t=1}^T \mathcal{L}_t^{(\text{val})}(\mathbf{a}_t^{(\mathcal{A}_i)}, \mathbf{a}_{-i}) - \min_{\mathbf{a} \in \{1, \dots, K\}} \left[\sum_{t=1}^T \mathcal{L}_t^{(\text{val})}(\mathbf{a}, \mathbf{a}_{-i}) \right] \right],$$

We want to relate that the game that agent i plays against an adversary when the actions of all the other agents are fixed to \mathbf{a}_{-i} to the vanilla EXP3 setting. To be more precise on why this is the EXP3 setting, first we have that $\mathcal{L}_t^{(\text{val})}(\mathbf{a}_t)$ is a function of \mathbf{a}_t that can take K^N arbitrary values. When we fix \mathbf{a}_{-i} , $\mathcal{L}_t^{(\text{val})}(\mathbf{a}_t^{(\mathcal{A}_i)}, \mathbf{a}_{-i})$ is a function of $\mathbf{a}_t^{(\mathcal{A}_i)}$ that can only take K arbitrary values.

One can redefine $\mathcal{L}_t^{\textcircled{a},(\text{val})}(\mathbf{a}_t^{(\mathcal{A}_i)}) = \mathcal{L}_t^{(\text{val})}(\mathbf{a}_t^{(\mathcal{A}_i)}, \mathbf{a}_{-i})$ and then the game boils down to the vanilla adversarial multi-arm bandit where each time the learner plays $\mathbf{a}_t^{(\mathcal{A}_i)} \in \{1, \dots, K\}$ and observes/incurs the loss $\mathcal{L}_t^{\textcircled{a},(\text{val})}(\mathbf{a}_t^{(\mathcal{A}_i)})$. Said differently this defines a game where the new ν' contains all the losses as $\nu' = \{\mathcal{L}_t^{\textcircled{a},(\text{val})}(\mathbf{a}_t^{(\mathcal{A}_i)})\}_{t \in \{1, \dots, T\}, \mathbf{a}_t^{(\mathcal{A}_i)} \in \{1, \dots, K\}}$.

For all \mathbf{a}_{-i}

$$\mathcal{R}_T^{*,i}(\text{EXP3}, \mathbf{a}_{-i}) \leq 2\sqrt{TK \log(K)}$$

Then we have

$$\begin{aligned} \mathcal{R}_T^{*,i}(\text{EXP3}) &\leq \sup_{\mathbf{a}_{-i}} 2\sqrt{TK \log(K)} \\ &= 2\sqrt{TK \log(K)} \end{aligned}$$

Then we have

$$\sum_{i=1}^N \mathcal{R}_T^{*,i}(\text{EXP3}) \leq 2N\sqrt{TK \log(K)}$$

□

E Relation between weight sharing and cumulative regret

Ideally we would like to obtain for any given architecture \mathcal{Z} the value $\mathcal{L}_{\text{val}}(\mathcal{Z}, \mathbf{w}^*(\mathcal{Z}))$. However obtaining $\mathbf{w}^*(\mathcal{Z}) = \arg \min_{\mathbf{w}} \mathcal{L}_{\text{train}}(\mathbf{w}, \mathcal{Z})$ for any given fixed \mathcal{Z} would already require heavy computations. In our approach the \mathbf{w}_t that we compute and update is actually common to all \mathcal{Z}_t as \mathbf{w}_t replaces $\mathbf{w}^*(\mathcal{Z}_t)$. This is a simplification that leads to learning a weight \mathbf{w}_t that tend to minimise the loss $\mathbb{E}_{\mathcal{Z} \sim \pi_t} [\mathcal{L}_{\text{val}}(\mathcal{Z}, \mathbf{w}(\mathcal{Z}))]$ instead of minimising $\mathcal{L}_{\text{val}}(\mathcal{Z}_t, \mathbf{w}(\mathcal{Z}_t))$. If π_t is concentrated on a fixed \mathcal{Z} then these two previous expressions would be close. Moreover when π_t is concentrated on \mathcal{Z} then \mathbf{w}_t will approximate accurately $\mathbf{w}^*(\mathcal{Z})$ after a few steps. Note that this gives an argument for using sampling algorithm that minimise the cumulative regret as they naturally tend to play almost all the time one specific architecture. However there is a potential pitfall of converging to a local minimal solution as \mathbf{w}_t might not have learned well enough to compute accurately the loss of other and potentially better architectures.